Article

Not peer-reviewed version

Apiol-Rich and Caryophyllene-Oxygenated Essential Oils from Amazonian Piper Species as Dual-Action Biopesticides: Broad-Spectrum and Selective Antifeedant

Liliana Ruiz-Vásquez *, Maria Fe Andrés Yeves, Mao Deng Jesulin Vela Mendoza, Lastenia Ruiz Mesia, Wilfredo Ruiz Mesia, Hivelli Ricopa Cotrina, Daniel Tapia, Félix Valcarcel, Azucena Gonzalez Coloma *

Posted Date: 22 May 2026

doi: 10.20944/preprints202605.1475.v1

Keywords: apiol; *Piper*; essential oil; antifeedant; ixodicidal; *Hyalomma lusitanicum*; *Spodoptera littoralis*; *Myzus persicae*; methylenedioxyphenyl; integrated pest management

 doi:10.20944/preprints202605.1475.v1

Article

Apiol-Rich and Caryophyllene-Oxygenated Essential Oils from Amazonian Piper Species as Dual-Action Biopesticides: Broad-Spectrum and Selective Antifeedant

Liliana RuizVásquez [1,2,*], Maria Fe Andrés Yeves [3], Mao Deng Jesulin Vela Mendoza [2], Lastenia Ruiz Mesia [1,4], Wilfredo Ruiz Mesia [1,4], Hivelli Ricopa Cotrina [1,4], Daniel Tapia [3], Félix Valcarcel [5] and Azucena Gonzalez Coloma [3,*]

[1] Laboratorio de Productos Naturales Antiparasitarios de la Amazonia, Centro de Investigación de Recursos Naturales, Universidad Nacional de la Amazonia Peruana (UNAP), Iquitos 16002, Peru
[2] Facultad de Farmacia y Bioquímica, Universidad Nacional de la Amazonia Peruana (UNAP), Iquitos 16000, Perú
[3] Instituto de Ciencias Agrarias, CSIC, 28006 Madrid, Spain
[4] Facultad de Ingeniería Química, Universidad Nacional de la Amazonia Peruana (UNAP), Iquitos 16000, Peru
[5] Reproducción Animal, INIA, CSIC., 28040 Madrid
* Correspondence: liliana.ruiz@unapiquitos.edu.pe (L.R.V.); azu@ica.csic.es (A.G.C.); Tel.: +51-966-102-718 (L.R.V.); +34-917-452-500 (A.G.C.)

Abstract

The increasing resistance of agricultural pests and disease-vectoring arthropods to synthetic pesticides highlights the need for novel, sustainable biocidal agents. This study evaluates, for the first time, the insect antifeedant and ixodicidal activities of essential oils from ten Amazonian *Piper* species and their major components. Antifeedant effects were tested against *Spodoptera littoralis, Myzus persicae,* and *Rhopalosiphum padi*, ixodicidal activity against *Hyalomma lusitanicum* larvae and their effects on the plant parasitic nematode *Meloidogyne javanica*. Essential oils from *P. mituense* (51.6% apiol) and *P. sancti-felicis* (76.1% apiol) showed the highest activity, achieving >75% inhibition across all insect species and 100% tick mortality. *P. mituense* consistently exhibited greater potency, suggesting synergistic effects from minor constituents. Principal component analysis associated apiol-rich chemotypes with broad-spectrum activity. In contrast, oils rich in oxygenated caryophyllene derivatives, particularly from *P. casapiense*, showed strong but selective antifeedant effects against *R. padi*. Pure apiol was active across all assays, while no nematicidal effects were detected. Molecular docking supported these findings, indicating that apiol can interact with acetylcholinesterase and cytochrome P450 targets. These results identify complementary *Piper* chemotypes with potential as dual-purpose biopesticides for integrated pest management.

Keywords: apiol; *Piper*; essential oil; antifeedant; ixodicidal; *Hyalomma lusitanicum*; *Spodoptera littoralis*; *Myzus persicae*; methylenedioxyphenyl; integrated pest management

1. Introduction

Resistance to synthetic pesticides in crop pests and disease transmitting arthropods demands alternative control strategies [1]. Key resistant species include the polyphagous lepidopteran *Spodoptera littoralis* (Boisduval), with documented resistance to pyrethroids, organophosphates, and spinosad [2]; the aphid vectors *Myzus persicae* (Sulzer), which has developed resistance to more insecticide classes than any other herbivorous arthropod [3], and *Rhopalosiphum padi* (L.) [4,5]; and

 doi:10.20944/preprints202605.1475.v1

the tick *Hyalomma lusitanicum* Koch principal reservoir/vector of Crimean, Congo hemorrhagic fever virus (CCHFV) in southwestern Europe [6–10]. These species collectively illustrate how multi-class resistance compromises conventional chemical control [1,3,10], highlighting the urgency of identifying new biocidal agents effective against both agricultural pests and arthropod vectors of public health concern.

Essential oils (EOs) from aromatic plants have emerged as promising candidates for sustainable pest management owing to their rapid biodegradability, low mammalian toxicity, and multiple simultaneous modes of action, targeting the octopaminergic system, GABA receptors, and acetylcholinesterase, which reduce selection pressure for resistance [11–15]. Among plant-based strategies, the antifeedant approach is particularly valuable for integrated pest management (IPM) by modulating contact chemoreception rather than exerting direct lethal toxicity, and lowering resistance risk [16,17].

The genus *Piper* L. (Piperaceae), with approximately 2000 tropical species, produces a remarkable diversity of essential oils rich in terpenoids and phenylpropanoids with pesticidal properties [18–20]. Of particular interest are phenylpropanoids bearing the methylenedioxyphenyl (MDP) pharmacophore, the same structural motif present in the synergist piperonyl butoxide (PBO), which inhibits cytochrome P450 monooxygenases involved in insect detoxification [21]. Dillapiole, the dominant MDP, phenylpropanoid in *Piper aduncum* L., has been extensively studied as an insecticide and acaricide [22], and safrole from *P. hispidinervum* C. DC. has shown antifeedant activity against *S. littoralis*, *M. persicae*, and *R. padi* with documented synergistic interactions [23]. In contrast, apiol (2,5-dimethoxy-3,4-methylenedioxy-1-allylbenzene), another MDP-bearing phenylpropanoid that dominates the essential oil of several *Piper* species, has received comparatively little attention despite sharing the same pharmacophore. To the best of our knowledge, neither the antifeedant nor the ixodicidal activities of apiol have been systematically evaluated, and no previous study has compared these activities across apiol-rich *Piper* chemotypes.

In a previous study, our group characterized the GC-MS composition, antifungal activity against *Botrytis cinerea*, and herbicidal potential of essential oils from ten *Piper* species collected in the Peruvian Amazon [24]. The essential oils exhibited diverse chemotypes: two species were dominated by apiol (*P. sancti-felicis*, 76.1%; *P. mituense*, 51.6%), while others were characterized by sesquiterpene hydrocarbons (β bisabolene, caryophyllene, germacrene D, bicyclogermacrene) or the monoterpene limonene. Three essential oils (*P. casapiense*, *P. soledadense*, and *P. mituense*) were described for the first time, and dillapiole was not detected in any of the ten essential oils [24], making apiol the sole dominant MDP-bearing compound in this collection. However, the insect antifeedant and ixodicidal potential of these essential oils and their dominant compound apiol was not investigated.

Phenylpropanoid, are a large and structurally diverse class of plant secondary metabolites involved in ecological interactions such as defense against herbivores, pathogens, and environmental stress [25,26]. Apiol, a benzodioxole-type phenylpropanoid, is widely distributed in plant essential oils and has been associated with several biological activities, including specific inhibitory effects on aflatoxin G_1 biosynthesis in *Aspergillus parasiticus* [27].

Accordingly, the aim of the present study was to evaluate, for the first time, the antifeedant effects of these ten Amazonian *Piper* essential oils and their main components against three model pest species (*S. littoralis*, *M. persicae*, and *R. padi*), together with their ixodicidal activity against *H. lusitanicum* larvae and additionally, their effects on the plant parasitic nematode *Meloidogyne javanica* (Treub) Chitwood. This work expands the biocidal profile of these Amazonian essential oils beyond their previously reported antifungal and herbicidal activities [24], contributing to the identification of apiol-rich *Piper* chemotypes as dual purpose biopesticidal agents for integrated management of crop pests and ticks. Additionally, molecular docking, a widely used computational method that predicts ligand–protein binding by sampling conformations and ranking them using scoring functions [28,29] has been used to compare the interactions of apiol versus known ligands on acetylcholinesterase and CYP450 proteins from insects, ticks and nematodes [30], to better understand the mechanism of action of apiol and the apiol-rich essential oils.

 doi:10.20944/preprints202605.1475.v1

2. Results

2.1. Essential Oil Composition

Table 1 shows the summarized chemical composition of the *Piper* essential oils studied here determined by GC-MS. Their chemical composition was previously reported [24]. Based on their dominant chemical classes, the essential oils were classified into four chemotypes: (i) a phenylpropanoid chemotype dominated by apiol (*P. sanctifelicis*, 76.1%; *P. mituense*, 51.6%); (ii) a predominantly monoterpene chemotype rich in limonene (*P. soledadense*, 38.5%); (iii) a bisabolene-type sesquiterpene chemotype (*P. coruscans*, β-bisabolene 33.4%; *P. tuberculatum*, β-bisabolene 40.2%); and (iv) a mixed sesquiterpene chemotype characterized by varying proportions of caryophyllenes (*P. anonifolium*), germacrene D, and bicyclogermacrene (*P. obliquum*, *P. dumosum*, *P. reticulatum*, and *P. casapiense*). In this work, further chemical identification of previously unidentified compounds has been carried out based on retention index and EI mass spectrum (see table S1 in supplementary information).

Three major (>5%) compounds have been identified in *P. casapiense*. Compounds eluting at rt 19.49 and 21.13 min (RI = 1711 and 1798) were dominated by ions at m/z 93, 91, 105 and 133, characteristic of caryophyllane-type fragmentation. These compounds have been tentatively identified as caryophyllenone and β-caryophyllenol. A third oxygenated caryophyllane derivative (rt 21.55 min) was detected with a retention index of 1821. Its EI mass spectrum was dominated by characteristic caryophyllane ions at m/z 93, 91, 105 and 133, together with additional fragments at m/z 107, 119 and 121, indicative of a higher degree of oxygenation. Based on its elevated retention index and fragmentation pattern, this compound was tentatively identified as a caryophyllane type diol or highly oxygenated caryophyllenol derivative. Its co-occurrence with caryophyllenone and β caryophyllenol supports a sequential oxidative transformation of a common β caryophyllene precursor within the essential oil. Similarly, in *P. anonifolium*, the EI mass spectrum (m/z 161/105/81/204/119/162/134/91/159/131) of compound eluting at rt 15.32 min and RI 1503 was characteristic of a caryophyllane alcohol. Additionally, in *P. obliquum*, the EI mass spectrum (m/z 95/121/161/204/43/109/105/81/164/108) of the compound eluting at rt 18.46 min and RI 1658 was characteristic of a highly oxygenated caryophyllane-type sesquiterpene (diol derivative).

Table 1. Major components (≥5%) of the essential oils from ten Amazonian *Piper* species.

Species	Major components (≥5%)
P. anonifolium	β-Caryophyllene (11.3%), germacrene D (9.6%), caryophyllane-type sesquiterpene (9.2%), δ-cadinene (6.6%), α-humulene (6.6%), (−)-β-copaene (5.8%), *cis*-β-copaene (5.8%), neoalloocimene (5.5%)
P. casapiense	β-Caryophyllenol (22%), β-caryophyllene oxide (10.2%), caryophyllane-type diol (5.4%)
P. coruscans	β-Bisabolene (33.4%), nerolidol (10.2%), β-caryophyllene (8%), (+)-β-Selinene (5%)
P. dumosum	Bicyclogermacrene (16.5%), germacrene D (10.4%), dillapiol (8.9%), β-caryophyllene (6.8%), β-pinene (6.3%), α-cubebene (5.9%), myristicin (3.7%)
P. mituense	Apiol (51.6%), bicyclogermacrene (9.0%), germacrene D (6.7%), dillapiol (5.3%), myristicin (4.6%)
P. obliquum	Bicyclogermacrene (7.9%), highly oxygenated caryophyllane-type sesquiterpene (7.7%), 10-epi-elemol (7.3%), caryophyllene oxide (6.3%), β-caryophyllene (6.3%), α-pinene (6%), β-pinene (5.1%)
P. reticulatum	Apiol (15%), germacrene D (12.6%), bicyclogermacrene (8.1%), δ-cadinene (6%)

 doi:10.20944/preprints202605.1475.v1

P. sancti-felicis	Apiol (76.1%)
P. soledadense	Limonene (38.5%), caryophyllene oxide (13.3%), γ-muurolene (5.8%)
P. tuberculatum	β-Bisabolene (40.2%), δ-cadinene (9.8%), β-caryophyllene (9.7%), germacrene D (5%)

2.2. Bioactivity

The insect antifeedant effects of the tested essential oils are shown in Table 2. The most sensitive insects were the aphids *M. persicae* (7 active of 10), *R. padi* (6 active of 10) and the lepidopterous *S. littoralis* (3 active of 10). Regarding insect species selectivity, *P. mituense* and *P. sancti-felicis* were active against all three insect species, *P. anonifolium, P. casapiense, P. obliquum* and *P. reticulatum* had significant effects on both aphid species, *P. coruscans* and *P. tuberculatum* were only active on *M. persicae* and *P. soledadense* on *R. padi*. The most active oil on *R. padi* was *P. casapiense* (EC_{50}, 3.8 μg/cm²), followed by *P. sancti-felicis* (EC_{50}, 8.6 μg/cm²), *P. mituense* (EC_{50}, 9.7 μg/cm²) and *P. obliquum* (EC_{50}, 25.6 μg/cm²), while *P. soledadense* and *P. anonifolium* had significant effect but did not reach the 70% inhibition threshold to carry out dose-response experiments. On *M. persicae, P. reticulatum* was the most active (EC_{50}, 16.2 μg/cm²) followed by *P. mituense* (EC_{50}, 23.2 μg/cm²), *P. tuberculatum* (EC_{50}, 39.5 μg/cm²) and *P. sancti-felicis* (EC_{50}, 53.5 μg/cm²), while *P. anonifolium, P. casapiense, P. coruscans* and *P. obliquum* had significant effect but did not reach the 70% inhibition threshold to carry out dose-response experiments. On *S. littoralis*, *P. mituense* (EC_{50}, 15.6 μg/cm²) was very active, followed by *P. sancti-felicis* (EC_{50}, 42.0 μg/cm²) and *P. dumosum*, with a feeding inhibition value below the 70% inhibition threshold.

Among the major components of the oils (Table 1), the following compounds were tested: apiol, β-bisabolene, δ-cadinene, β-caryophyllene, β-caryophyllene oxide, germacrene D, α-humulene, limonene, nerolidol, β-pinene, α-pinene (Table 2). Additionally, myristicin was included because of its potential synergistic action.

Apiol was active against the three insect targets with EC_{50} values of 22.24, 16.00 and 17.70 μg/cm² against *S. littoralis, M. persicae* and *R. padi* respectively. Nerolidol showed significant effects on both aphid species and α-pinene on *S. littoralis* but did not reach the 70% inhibition threshold to carry out dose-response experiments (Table 2).

The ten essential oils and apiol were also evaluated for nematicidal activity against *Meloidogyne javanica* second stage juveniles (J2). None of the essential oils nor the pure compound exhibited significant nematicidal effects at the concentrations tested (see Table S2).

Table 2. Antifeedant effects of the essential oils from *Piper* species, the main components of the active oils and myristicin on *S. littoralis*, *M. persicae*, and *R. padi*.

Species/compounds	**%FI-SI[a] / EC_{50} [b]**	***S. littoralis***	***M. persicae***	***R. padi***
P. anonifolium	%FI-SI	30 ± 8	69 ± 5*	52 ± 8*
	EC_{50}	>50	~50	~50
P. casapiense	%FI-SI	12 ± 8	67 ± 7*	76 ± 5*
	EC_{50}	>50	~50	3.8 (1.6-8.8)
P. coruscans	%FI-SI	40 ± 5	74 ± 5*	34 ± 7
	EC_{50}	>50	~50	>50
P. dumosum	%FI-SI	58 ± 12*	32 ± 8	40 ± 8
	EC_{50}	~50	>50	>50
P. mituense	%FI-SI	91 ± 3*	91 ± 3*	92 ± 4*
	EC_{50}	15.6 (8.7-27.8)	23.2 (19.1-28.3)	9.7 (5.6-16.9)
P. obliquum	%FI-SI	21 ± 9	58 ± 7*	89 ± 3*
	EC_{50}	>50	~50	25.6 (17.6-35.4)
P. reticulatum	%FI-SI	26 ± 13	90 ± 4*	62 ± 6*

 doi:10.20944/preprints202605.1475.v1

	EC_{50}	>50	16.2 (9.2-28.5)	~50
P. sancti-felicis	%FI-SI	90 ± 4*	79 ± 5*	97 ± 1*
	EC_{50}	42.0 (35.3-49.8)	53.5 (40.6-70.5)	8.6 (5.6-13.4)
P. soledadense	%FI-SI	48 ± 13	44 ± 9	56 ± 7
	EC_{50}	>50	>50	~50
P. tuberculatum	%FI-SI	9 ± 6	77 ± 5*	39 ± 7
	EC_{50}	>50	39.5 (29.1-58.0)	>50
Apiol	%FI	81.84 ± 11.00*	95.32 ± 1.59*	99.07 ± 0.93*
	EC_{50}	22.24 (16.27-29.73)	16.00 (11.09-21.85)	17.70 (14.79-21.78)
β-Bisabolene	%FI	29.94 ± 16.16	-	-
	EC_{50}	>50	-	-
δ-Cadinene	%FI	16.24 ± 11.02	-	-
	EC_{50}	>50	-	-
β-Caryophyllene	%FI	17.02 ± 10.44	26.7 ± 7.28	46.71 ± 7.78
	EC_{50}	>50	>50	>50
β-Caryophyllene oxide	%FI	55.20 ± 12.90*	24.63 ± 7.66	24.69 ± 7.20
	EC_{50}	~50	>50	>50
α-Humulene	%FI	29.99 ± 15.79	-	-
	EC_{50}	>50	-	-
Limonene	%FI	26.14 ± 8.69	38.39 ± 8.77	31.47 ± 7.12
	EC_{50}	>50	>50	>50
Myristicin	%FI	66.93 ± 9.80*	-	-
	EC_{50}	~50	-	-
Nerolidol[c]	%FI	25.91 ± 16.44	60.94 ± 10.3*	54.02 ± 8.34*
	EC_{50}	>50	≅50	≅50
β-Pinene	%FI	30.87 ± 7.67	35.04 ± 7.49	34.63 ± 6.27
	EC_{50}	>50	>50	>50
α-Pinene	%FI	49.16 ± 16.18	26.61±7.50	23.25 ± 5.74
	EC_{50}	>50	>50	>50

[a] %FI-SI = [1-(T/C)] x 100, where T and C are the consumption/settling of treated and control leaf disks, respectively. [b] Effective antifeedant dose (EC_{50}) and 95% confidence (lower, upper) (μg/cm²). [c] Ref. [31]. *Significantly different from the control, P>0.05, Wilcoxon signed rank test.

Table 3 shows the ixodicidal activity of the ten *Piper* essential oils against *Hyalomma lusitanicum* larvae. Five essential oils were effective ixodicidal agents, with *P. mituense* being the most active (LD_{50} = 1.46 μg/mg cellulose), followed by *P. sanctifelicis* (LD_{50} = 2.14 μg/mg cellulose), *P. reticulatum* (LD_{50} = 6.19 μg/mg cellulose), *P. dumosum* (LD_{50} = 8.89 μg/mg cellulose), and *P. soledadense* (LD_{50} = 10.05 μg/mg cellulose).

The major components of the active oils (apiol, limonene, α- and β-pinene, caryophyllene, β-caryophyllene oxide, nerolidol, copaene and δ-cadinene) were tested on *H. lusitanicum* larvae (Table 3). Myristicin was also included similarly to the tests on insects. Apiol (LD_{50} of 1.96 μg/mg cellulose) and β-caryophyllene oxide (LD_{50} of 4.46 μg/mg cellulose) and myristicin (LD_{50} of 2.88 μg/mg cellulose) were active (Table 3).

Table 3. Ixodicidal activity of *Piper* oils, the main components of the active oils and myristicin against *Hyalomma lusitanicum* larvae.

Essential oil	**Mortality[a]**	**LD_{50} [μg/mg cellulose]**	**LD_{90} [μg/mg cellulose]**
P. anonifolium	35 ± 8	>40	>40
P. casapiense	53 ± 7	>40	>40

 doi:10.20944/preprints202605.1475.v1

P. coruscans	42 ± 19	>40	>40
P. dumosum	100 ± 0	8.891 (8.304-9.600)	13.813 (12,619-15.566)
P. mituense	100 ± 0	1.457 (1.323-1.616)	2.171 (1.962-2.469)
P. obliquum	38 ± 5	>40	>40
P. reticulatum	100 ± 0	6.190 (5.564-6.884)	9.684 (8.733-11.077)
P. sancti-felicis	100 ± 0	2.139 (1.899-2.372)	3.543 (3.219-4.010)
P. soledadense	100 ± 0	10.055 (9.089-11.077)	16.729 (15.066-19.343)
P. tuberculatum	7 ± 2	>40	>40
Apiol	100 ± 0	1.966 (1.798-2.162)	6.321 (5.601-7.671)
δ-Cadinene	0	>20	>20
Caryophyllene	19.4 ± 9.52	>20	>20
β-Caryophyllene oxide	100	4.462 (4.020-5.044)	6.321 (5.601-7.671)
Copaene	0	>20	>20
Limonene	6.8 ± 1.84	>20	>20
Myristicin	100	2.885 (2.613-3.198)	4.452 (4.032-5.037)
Nerolidol	10.97 ± 2.01	>20	>20
α-Pinene	0	>20	>20
β-Pinene	0	>20	>20

[a] Mortality values (mean ± standard error) were corrected according to *Schneider Orelli* formula (at a dose of 20 and 10* µg/mg cellulose).

2.3.1. Principal Component Analysis

Principal component analysis was performed on a matrix of 26 active variables (23 compounds with relative abundance ≥5% in at least one species and three antifeedant EC_{50} values) across the ten *Piper* species, using autoscaling. The first two principal components accounted for 21.9% and 18.3% of the total variance, respectively (40.2% cumulative), and their biplot is shown in Figure 1.

The score plot revealed three distinct groupings. The apiol-rich species *P. mituense* (Pm) and *P. sancti-felicis* (Psf) clustered in the upper-left quadrant, driven by the strong positive loading of apiol on PC2 and its negative contribution to PC1. In contrast, the β-bisabolene-dominated species *P. coruscans* (Pc) and *P. tuberculatum* (Pt) were projected into the lower-center region, associated with the loadings of β-bisabolene, δ-cadinene, nerolidol, and β-caryophyllene. The sesquiterpene-rich species *P. anonifolium* (Pa) and *P. dumosum* (Pd) occupied the right side of the plot, separated along PC1 by high loadings of germacrene D, α-cubebene, and α-humulene. *P. casapiense* (Pcs) was clearly isolated in the lower-left quadrant, driven by oxygenated caryophyllane derivatives (caryophyllenone, β-caryophyllenol, caryophyllane oxide, and oxygenated caryophyllane diol), which are exclusive to this species. *P. soledadense* (Ps) occupied an intermediate position in the left-center region, consistent with its limonene-dominated monoterpene chemotype. *P. obliquum* (Po) and *P. reticulatum* (Pr) were positioned near the center, reflecting their mixed sesquiterpene profiles without a single dominant compound.

The projection of the antifeedant EC_{50} variables (red arrows, Figure 1) provided insight into the relationship between chemical composition and biological activity. The EC_{50} vectors for *S. littoralis* (Sl) and *M. persicae* (Mp) pointed toward the center-right of the plot, while the EC_{50} vector for *R. padi* (Rp) was directed toward the lower-left quadrant. Since lower EC_{50} values indicate greater antifeedant potency, the most active species are those projected in the direction opposite to the EC_{50} vectors. Accordingly, Pm and Psf, located opposite to all three EC_{50} vectors, were associated with the strongest broad-spectrum antifeedant activity, consistent with their apiol-rich chemotype. The proximity of the apiol loading vector to these species and its opposition to the EC_{50} vectors confirmed

 doi:10.20944/preprints202605.1475.v1

that apiol content is the primary chemical determinant of broad-spectrum antifeedant efficacy. Conversely, the sesquiterpene-dominated species (Pa, Pc, Pt) were projected near or along the EC_{50} vectors, consistent with their weak or absent antifeedant effects. *P. casapiense* (Pcs), despite its position opposite to the Rp vector, showed strong selective activity against *R. padi* (EC_{50} = 3.8 μg/cm²), suggesting that its oxygenated caryophyllane derivatives may contribute to taxon-selective antifeedant effects.

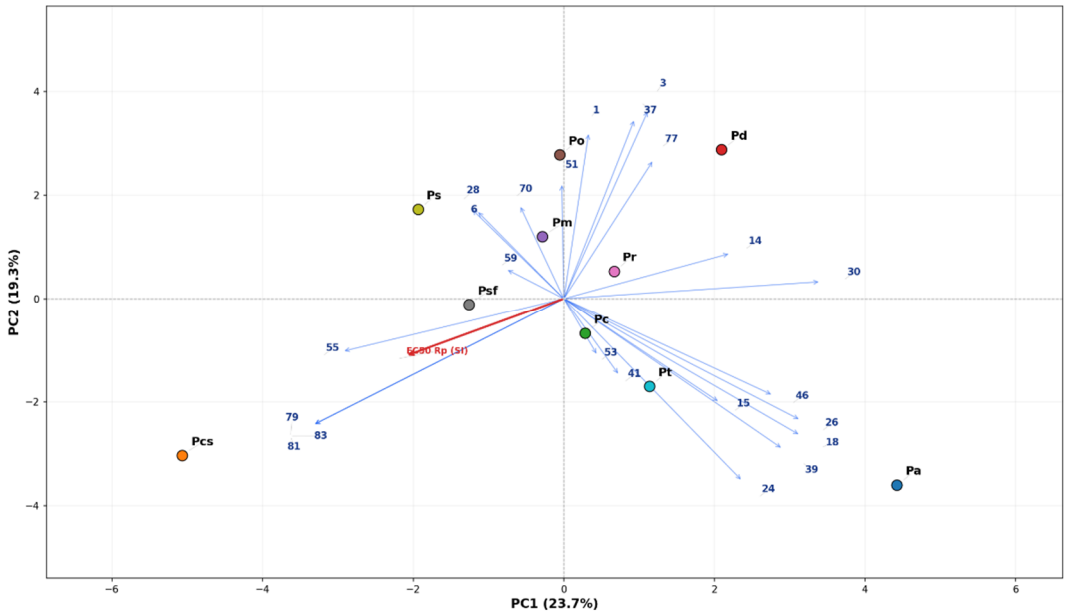

Figure 1. PCA biplot integrating the chemical composition and antifeedant activity against *Rhopalosiphum padi* (Sl) of essential oils from ten Amazonian *Piper* species (23 compounds with relative abundance ≥5% and EC_{50}; autoscaled). Blue arrows represent compound loadings; red arrows represent EC_{50} values, with direction inverted so that the vectors point toward the most active species (lower EC_{50} = higher activity). PC1 and PC2 explain 23.7% and 19.3% of the total variance, respectively (43.0% cumulative). Species abbreviations: Pa = *P. anonifolium*; Pcs = *P. casapiense*; Pc = *P. coruscans*; Pd = *P. dumosum*; Pm = *P. mituense*; Po = *P. obliquum*; Pr = *P. reticulatum*; Psf = *P. sancti-felicis*; Ps = *P. soledadense*; Pt = *P. tuberculatum*. Compound numbers correspond to their elution order in the GC-MS database (Table S1): **1** = α-pinene; **3** = β-pinene; **6** = limonene; **14** = α-cubebene; **15** = cis-β-copaene; **18** = β-caryophyllene; **24** = α-humulene; **26** = neoalloocimene; **28** = γ-muurolene; **30** = germacrene D; **37** = bicyclogermacrene; **39** = caryophyllane alcohol isomer II; **41** = β-bisabolene; **46** = δ-cadinene; **51** = 10-epi-elemol; **53** = nerolidol; **55** = caryophyllene oxide; **59** = apiol; **70** = highly oxygenated caryophyllane-type sesquiterpene diol derivative; **77** = dillapiol; **79** = caryophyllenone; **81** = β-caryophyllenol; **83** = caryophyllane-type diol.

A second PCA (Figure 2) was performed on a matrix of 24 active variables (23 compounds with relative abundance ≥5% in at least one species and the LD_{50} against *H. lusitanicum* larvae) across the ten *Piper* species, using autoscaling. PC1 and PC2 explained 22.0% and 19.1% of the total variance, respectively (41.1% cumulative). The LD_{50} vector (red arrow) pointed toward the upper-left quadrant, where the five ixodicidally active species were clustered: *P. mituense* (Pm, LD_{50} = 1.46 μg/mg), *P. sancti-felicis* (Psf, LD_{50} = 2.14 μg/mg), *P. reticulatum* (Pr, LD_{50} = 6.19 μg/mg), *P. dumosum* (Pd, LD_{50} = 8.89 μg/mg), and *P. soledadense* (Ps, LD_{50} = 10.06 μg/mg). The apiol loading vector was co-directional with the LD_{50} vector and closely aligned with Pm and Psf, the two most potent species, confirming that apiol is the primary driver of ixodicidal activity, in agreement with the high potency of pure apiol (LD_{50} = 1.97 μg/mg, Table 3). Notably, Pd was projected in the upper quadrant alongside the dillapiol, bicyclogermacrene, and β-pinene vectors, suggesting that its ixodicidal activity (100% mortality) may be attributable to dillapiol (8.9%) and myristicin (3.7%), both MDP-bearing compounds, rather than to its sesquiterpene background. This contrasted with the antifeedant PCA

 doi:10.20944/preprints202605.1475.v1

(Figure 1), where Pd failed to achieve broad-spectrum activity, indicating that the MDP-phenylpropanoid threshold for ixodicidal effects may be lower than that required for antifeedant efficacy.

In contrast, the inactive species (LD_{50} > 40 µg/mg) were projected in the opposite region of the biplot. *P. anonifolium* (Pa) was isolated in the far right, driven by α-humulene, β-caryophyllene, caryophyllane alcohol isomer II, and neoalloocimene loadings, while *P. coruscans* (Pc) and *P. tuberculatum* (Pt) clustered in the lower-center region along the β-bisabolene and δ-cadinene vectors. Their position opposite to the LD_{50} vector was consistent with the absence of ixodicidal activity for pure β-caryophyllene, limonene, α-pinene, β-pinene, and copaene (all with LD_{50} > 20 µg/mg, Table 3). *P. casapiense* (Pcs) was again isolated in the lower-left quadrant by its exclusive oxygenated caryophyllane derivatives (caryophyllenone, β-caryophyllenol, caryophyllene oxide); despite its moderate mortality (53 ± 7%), it did not achieve a calculable LD_{50}, indicating that the oxygenated caryophyllane chemotype that conferred potent selective antifeedant activity against *R. padi* (Section 2.3.1) did not translate into equivalent ixodicidal effects. The only active non-apiol compound was β-caryophyllene oxide (LD_{50} = 4.46 µg/mg) and myristicin (LD_{50} = 2.89 µg/mg), whose individual contributions may partially explain the ixodicidal activity of Ps (caryophyllene oxide 13.3%) and Pr (apiol 15.0% combined with a mixed sesquiterpene profile).

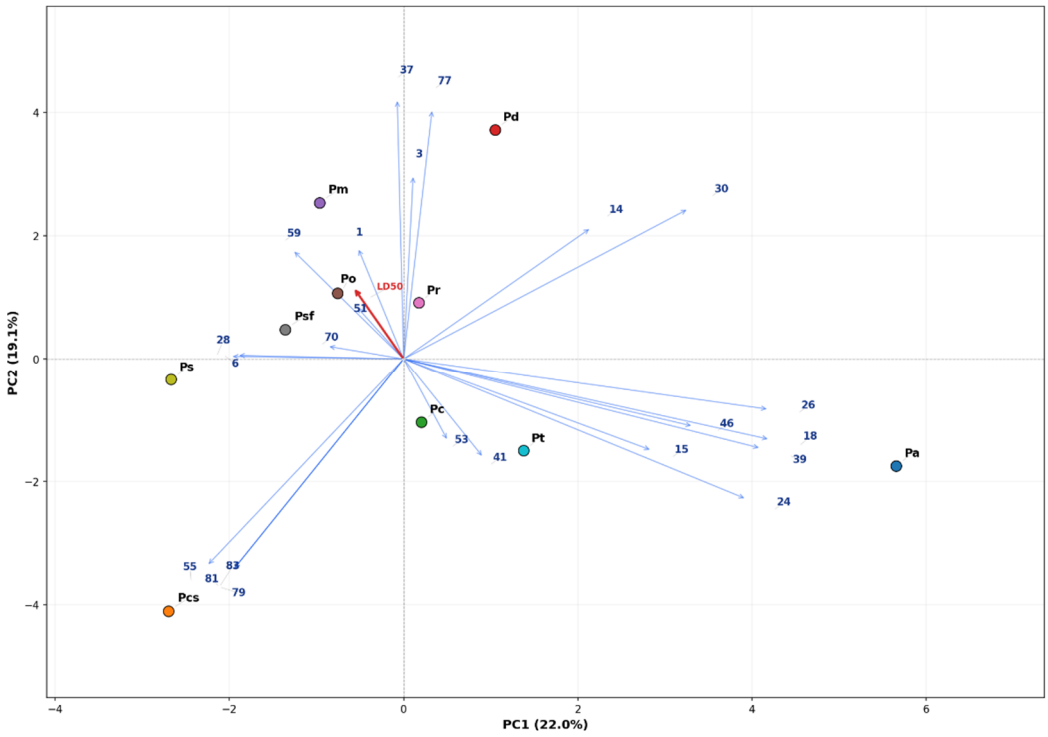

Figure 2. PCA biplot integrating the chemical composition and ixodicidal activity (LD_{50}) against *Hyalomma lusitanicum* larvae of essential oils from ten Amazonian Piper species (24 active variables: 23 compounds with relative abundance ≥5% + LD_{50}; autoscaled). Blue arrows represent compound loadings; the red arrow represents the LD_{50}, with direction inverted so that the vector points toward the most active species (lower LD_{50} = higher ixodicidal activity). PC1 and PC2 explain 22.0% and 19.1% of the total variance, respectively (41.1% cumulative). Species abbreviations: Pa = *Piper anonifolium*; Pcs = *P. casapiense*; Pc = *P. coruscans*; Pd = *P. dumosum*; Pm = *P. mituense*; Po = *P. obliquum*; Pr = *P. reticulatum*; Psf = *P. sancti-felicis*; Ps = *P. soledadense*; Pt = *P. tuberculatum*. Compound numbers correspond to their elution order in the GC-MS analysis (Table S1): **1** = α-pinene; **3** = β-pinene; **6** = limonene; **14** = α-cubebene; **15** = cis-β-copaene; **18** = β-caryophyllene; **24** = α-humulene; **26** = neoalloocimene; **28** = γ-muurolene; **30** = germacrene D; **37** = bicyclogermacrene; **39** = caryophyllane alcohol isomer II; **41** = β-bisabolene; **46** = δ-cadinene; **51** = 10-epi-elemol; **53** = nerolidol; **55** = caryophyllene oxide; **59** = apiol; **70** = highly oxygenated caryophyllane-type sesquiterpene diol derivative; **77** = dillapiol; **79** = caryophyllenone; **81** = β-caryophyllenol; **83** = caryophyllane-type diol.

 doi:10.20944/preprints202605.1475.v1

2.3.2. Docking

Apiol demonstrated binding affinities comparable to or better than those of reference ligands across several targets (Figure 3, Supplementary Table S3). In AChE enzymes, improved binding was observed in *S. littoralis* and *Ixodes scapularis*, whereas slightly reduced affinity was found in *M. persicae* and *M. javanica*. In CYP450 enzymes, apiol showed improved binding in *Drosophila melanogaster* relative to α-pinene but slightly reduced affinity in *H. asiaticum* compared to terpinolene.

Apiol maintained interactions with catalytic residues in AChE. The interactions with the Ser and His of the catalytic triad were consistent across the generated poses. Also, the same interactions of acetylcholine with non-catalytic residues were detected in the case of apiol, indicating proper positioning within the active site (Supplementary Table S1). Additional interactions not observed in control ligands were identified, suggesting alternative stabilization mechanisms within the binding pocket. In the case of *D. melanogaster*'s CYP450, only the interaction with the catalytic Ile was detected, nonetheless, other non-catalytic interactions were shared between the reference ligand and apiol, suggesting the compatibility of the molecule with the binding position.

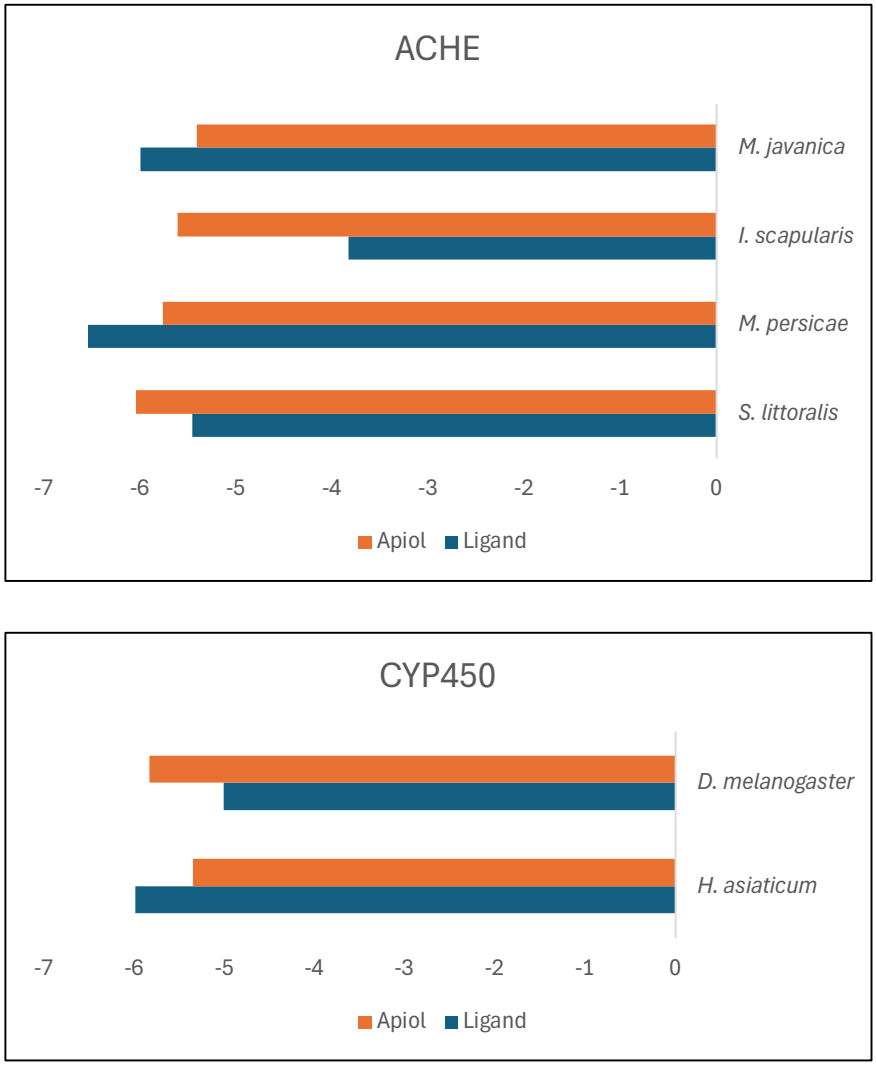

Figure 3. A: Comparative docking scores of apiol and acetylcholine in acetylcholinesterase (AChE) from four target species. Bar plots represent the best (lowest) docking scores obtained from 50 generated poses for each ligand–protein pair. Species included are *Spodoptera littoralis, Myzus persicae, Ixodes scapularis*, and *Meloidogyne javanica*. More negative values indicate stronger predicted binding affinity. **B:** Docking score comparison of apiol and reference ligands in cytochrome P450 enzymes. Bar plots show the best docking scores for apiol and species-specific reference ligands: terpinolene for *Hyalomma asiaticum* CYP3A8 and α-pinene for *Drosophila melanogaster* CYP6A2. Values correspond to the most favorable pose among 50 generated conformations.

 doi:10.20944/preprints202605.1475.v1

3. Discussion

The present study demonstrates that apiol-rich essential oils from Amazonian *Piper* species exhibit strong and consistent biocidal activity across both insect pests and ticks, supporting their potential as dual-purpose agents for integrated pest management.

The broad-spectrum antifeedant activity observed for *P. mituense* and *P. sancti-felicis*, together with their high ixodicidal efficacy and the strong correlation between apiol content and biological activity revealed by PCA highlights the central role of apiol as a key determinant of bioactivity. This finding is consistent with the ecological function of phenylpropanoids in plant defense, where these metabolites contribute to herbivore deterrence and protection against biotic stress [25,26].

A notable exception to the apiol-driven pattern was *P. casapiense*, which exhibited the strongest selective antifeedant activity against *R. padi* despite lacking high apiol content. This species, characterized by a chemotype rich in oxygenated caryophyllene derivatives, particularly β-caryophyllenol, caryophyllenone, and related highly oxygenated caryophyllane-type compounds, was clearly separated in the PCA and positioned opposite to the *R. padi* EC_{50} vector. This indicates that its activity arises from a distinct chemical mechanism compared to apiol-rich oils. Oxygenated caryophyllane sesquiterpenes, particularly caryophyllene oxide, have been widely reported to exhibit multi-target bioactivity against insects, including larvicidal effects, oviposition deterrence, developmental disruption, and strong repellency, often exceeding the activity of the non-oxygenated parent compound β-caryophyllene [32–35]. A similar pattern was observed for *P. obliquum*, characterized by bicyclogermacrene, oxygenated caryophyllene derivatives, and other caryophyllene-related sesquiterpenes. Bicyclogermacrene exhibited potent larvicidal activity against mosquito larvae, including *Anopheles subpictus, Aedes albopictus,* and *Culex tritaeniorhynchus* [36]. Sesquiterpene-rich essential oils have been shown to interfere with insect feeding behavior and sensory perception, particularly in aphids, which rely heavily on contact chemoreception [17,37]. Therefore, in addition to apiol-mediated broad-spectrum activity, alternative chemotypes based on oxygenated caryophyllenes and related sesquiterpenes can confer potent but selective antifeedant effects.

The observed differences between antifeedant and ixodicidal responses further suggest that distinct biological targets and thresholds may be involved. While high apiol content was required to achieve broad-spectrum antifeedant activity, ixodicidal effects were observed at lower concentrations, as evidenced by the activity of *P. dumosum*, which contains moderate amounts of MDP-bearing compounds such as dillapiol and myristicin.

At the molecular level, docking results provide mechanistic support for the experimental observations. Apiol exhibited similar or better binding affinities than endogenous ligands in acetylcholinesterase (AChE), suggesting that it may act as a competitive inhibitor. Since AChE plays a central role in neurotransmission by hydrolyzing acetylcholine, its inhibition leads to accumulation of the neurotransmitter and disruption of neural signaling, ultimately causing paralysis and death in insects [38,39]). The preservation of interactions with catalytic and non-catalytic residues supports the hypothesis that apiol binds within the active site and may interfere with enzymatic function.

In addition to AChE inhibition, apiol also showed relevant interactions with cytochrome P450 enzymes. Inhibition of cytochrome P450 monooxygenases is a mechanism well documented for methylenedioxyphenyl (MDP) phenylpropanoids such as apiol [40]. The variability observed across CYP450 targets reflects the structural diversity and functional adaptability of these enzymes, which are known to metabolize a wide range of xenobiotics [41]. Enhanced CYP450 activity is a major mechanism of insecticide resistance, allowing insects to degrade toxic compounds efficiently [42,43]. This structural motif is also present in piperonyl butoxide, a well-known synergist that inhibits cytochrome P450-mediated detoxification pathways in insects [21,44].

The dual interaction of apiol with both AChE and CYP450 enzymes is particularly relevant from an applied perspective. Multi-target compounds are less prone to resistance development because they simultaneously affect multiple physiological pathways [11,12]. In this context, apiol and apiol-rich essential oils may offer an advantage over single-target synthetic insecticides, aligning with

 doi:10.20944/preprints202605.1475.v1

current strategies aimed at reducing resistance pressure and improving sustainability in pest management.

The integration of chemical composition, bioactivity, and molecular docking data allows the identification of clear structure–activity relationships (SAR) within the essential oils of *Piper* species. Two major chemotypes emerge as biologically relevant: (i) apiol-rich phenylpropanoid systems, associated with broad-spectrum activity, and (ii) sesquiterpene-rich systems, particularly those dominated by oxygenated caryophyllenes, associated with selective antifeedant effects. Taken together, these findings support a dual SAR framework in *Piper* essential oils: (i) MDP-phenylpropanoids (apiol, dillapiol-like systems) confer broad-spectrum activity through combined AChE inhibition and CYP450 modulation; (ii) oxygenated sesquiterpenes (caryophyllene derivatives) confer selective antifeedant activity through behavioral and sensory interference mechanisms. This duality provides a mechanistic explanation for the diversity of biological responses observed and highlights the potential of combining different chemotypes to achieve both broad-spectrum and target-specific pest control strategies.

Overall, the combination of chemical, biological, and molecular docking data provides a comprehensive understanding of the activity of apiol-rich essential oils. The consistency between PCA, bioassays, and in silico results supports a unified mechanism in which apiol acts as a central bioactive compound, modulated by synergistic interactions and capable of targeting multiple physiological systems. The integration of chemical, biological, and computational data provides a comprehensive understanding of the activity of apiol-rich essential oils. Consistent results from PCA, bioassays, and molecular docking indicate that apiol is the main active compound, with its effects enhanced by synergistic interactions and its ability to target multiple physiological systems.

4. Materials and Methods

4.1. Plant Material and Essential Oil Extraction

The aerial parts (leaves, stems, and flowers) of ten *Piper* species were collected in three districts of the Loreto Department, Peruvian Amazon (Figure X): Mazán District (*P. coruscans*, voucher 039849; *P. casapiense*, 041044; *P. obliquum*, 027690; *P. anonifolium*, 042381; *P. tuberculatum*, 020115), Punchana District (*P. sancti,,felicis*, 036367), and San Juan Bautista District (*P. dumosum*, 040311; *P. reticulatum*, 042127; *P. soledadense*, 033308; *P. mituense*, 041473). Voucher specimens were deposited at the Herbarium AMAZ, Universidad Nacional de la Amazonia Peruana (UNAP), Iquitos, Peru. All plant material was collected under Regional Management Resolution No. 035, 2021, GRL, GGR, GRDFFS. Essential oils were obtained by hydrodistillation of the dried aerial parts, separated by decantation, and dried over anhydrous Na_2SO_4, yielding between 0.078% and 1.26% (dry weight basis). Collection coordinates, dry weights, and detailed extraction procedures have been previously reported [24].

4.2. Gas Chromatography–Mass Spectrometry (GC-MS) Analysis

The chemical composition of the essential oils was determined by GC,,MS using a Shimadzu GCMS, QP2010, Ultra system equipped with a Teknokroma TRB, 5 column (30 m × 0.25 mm ID, 0.25 µm film thickness) under the conditions previously described [24]. Compound identification was based on comparison of mass spectra with the Wiley 275 Mass Spectral Database and retention indices from the literature. Quantification was performed using relative peak area percentages. The complete chemical profiles of the ten essential oils, including three species described for the first time (*P. soledadense*, *P. casapiense*, and *P. mituense*), are detailed in [24] and summarized in Table 1 of the present work.

4.3. Antifeedant Bioassays

The colonies of *S. littoralis*, *M. persicae*, and *R. padi* were maintained at ICA, CSIC (Madrid, Spain) on artificial diet, bell pepper (*Capsicum annuum*), and barley (*Hordeum vulgare*), respectively (22 ± 1 °C, >70% RH, 16:8 h L:D). Antifeedant activity was evaluated using choice tests as previously

 doi:10.20944/preprints202605.1475.v1

described [45,46]. Feeding inhibition (%FI) against *S. littoralis* sixth, instar larvae (6 replicates, 2 larvae each) was calculated as %FI = [1 − (T/C)] × 100, where T and C are the consumption of treated and control leaf disks. Settling inhibition (%SI) against apterous adults of *M. persicae* and *R. padi* (22 replicates, 10 aphids each) was calculated as %SI = [1 − (%T/%C)] × 100, where %T and %C are the percentages of aphids on treated and control surfaces. The essential oils were tested at an initial concentration of 100 μg/cm². The pure compound apiol (Sigma, Aldrich, St. Louis, MO, USA) was tested under identical conditions.

4.4. Nematicidal Bioassays

The population of *M. javanica* was maintained at ICA, CSIC (Madrid, Spain) [47]. Egg masses of *M. javanica* were manually collected from infected tomato roots. Second-stage juveniles (J2) were obtained from hatched eggs by incubating handpicked egg masses in a water suspension at 25ºC for 24 h. The oils tested were dissolved in distilled water containing 5% of a DMSO-Tween solution (0.5% Tween 20 in DMSO) and evaluated at initial concentration of 1 μg/μL [47]. The control solution was distilled water/DMSO/ Tween 20. Each treatment was performed in quadruplicate. The plates were sealed and incubated in a growth chamber under the same conditions used for egg mass incubation. Dead J2s were counted at 72 h using a binocular microscope and mortality rate (M%) was calculated and corrected with Schneider-Orelli's formula [13].

4.5. Ixodicidal Bioassays

The engorged females of *H. lusitanicum* were collected from red deer in Ciudad Real (Central Spain) and maintained at 22–24 °C, 80% RH until larval hatching. Larvicidal bioassays were performed using the impregnated substrate method [46,48]. Test solutions (50 μL) were applied to 25 mg of powdered cellulose at initial concentrations of 20 μg/mg (essential oils) and 10 μg/mg (apiol). Three replicates of 20 larvae (>6 weeks old) were used per treatment. Negative (cellulose) and positive (thymol, 20 μg/mg) controls were included. Mortality was assessed after 24 h and corrected by the Schneider–Orelli formula [13].

4.6. Statistical Analysis

Antifeedant effects (%FI and %SI) were analyzed for significance using the non-parametric Wilcoxon signed rank test. Effective concentrations (EC_{50}) were determined by linear regression analysis (%FI or %SI vs. log dose) for essential oils exhibiting inhibition values ≥75% (Table 2). LD_{50} and LD_{90} values for the ixodicidal bioassays were calculated by Probit analysis using 1:2 serial dilutions covering a range between 100% and <50% mortality, with a minimum of three doses (Table 3). For *P. mituense*, the Probit regression yielded a negative LD_{50} estimate; a surrogate value (LOD/2) was assigned following established substitution methods for left ensored data [49,50]. EC_{50} calculations and Probit analyses were performed using STATGRAPHICS Centurion XVI (version 16.1.02).

Principal component analyses (PCA) were performed to explore the relationships between essential oil composition and biological activity. The antifeedant PCA included the 18 identified compounds and three EC_{50} variables as active variables. The ixodicidal PCA used the 18 identified compounds as active variables and the corrected mortality against *H. lusitanicum* as a supplementary variable. Statistical analyses and PCA visualizations were performed using Python (version 3.11.6). All computations were executed using the Julius computational platform (https://julius.ai/), which ensured reproducibility and standardization of the workflow.

4.7. Molecular Docking

The protein sequences of acetylcholinesterase were obtained from the UniProt database. The entries chosen were B7QEQ1 (*I. scapularis*) Q8T7U9 (*M. persicae*), A0A915MGH7 (*M. javanica*) and A0A9P0N5I4 (*S. littoralis*) (https://doi.org/10.1093/nar/gkae1010) . The protein CYP450 3A8 of *H.*

 doi:10.20944/preprints202605.1475.v1

asiaticum was obtained from Genbank (https://doi.org/10.1093/nar/gks1195) (entry: PQ058615.1) and the protein CYP450 6A2 of *D. melanogaster* was obtained from UniProt (entry: P33270). All the 3D models were generated using the SWISS-MODEL tool (https://doi.org/10.1093/nar/gky427).

Ligands were prepared using the OPLS4 force field, which provides enhanced accuracy in modeling molecular interactions and conformational energetics (Schrödinger, 2026). Ionization states were assigned using Epik, and stereochemistry was preserved. Protein structures were prepared at physiological pH (7.4). Hydrogen atoms were added and protonation states optimized to ensure proper representation of electrostatic interactions.

Docking grids were centered on active-site residues with a grid size of 20 Å. Fifty poses were generated for each ligand–protein pair and ranked based on docking score. Docking predicts the preferred binding orientation and affinity of ligands to protein targets through scoring functions (Sharmila et al., 2025). The best (lowest) docking score per system was selected. Interaction patterns were analyzed across all generated poses to identify conserved residues and unique contacts. Interaction types were assigned based on residue chemical properties and ligand orientation, considering standard criteria (hydrogen bonding, π–π stacking, hydrophobic and polar interactions) derived from docking poses.

4.7. Use of Generative Artificial Intelligence

In preparing this manuscript, the authors utilized AI, assisted tools (Claude Opus 4.6, Anthropic) to enhance the grammatical structure and linguistic clarity of the English writing, and Python, based PCA visualizations were generated with the assistance of Julius AI. All scientific content, experimental design, data collection, analysis, and interpretation represent the original intellectual contribution of the research team. No AI, assisted tools were used for data generation, scientific reasoning, or interpretation of results. The authors reviewed and take full responsibility for the accuracy and integrity of all content presented in this publication.

5. Conclusions

This study demonstrated, for the first time, that apiol-rich essential oils from Amazonian *Piper* species possess dual biopesticidal activity: broad-spectrum antifeedant effects against *S. littoralis*, *M. persicae*, and *R. padi* (EC_{50} 0.38–5.35 μg/cm²), and potent ixodicidal activity against *H. lusitanicum* larvae (LD_{50} 0.046–0.267 μg/mg cellulose). Among the ten species evaluated, *P. mituense* and *P. sancti-felicis*—both dominated by the phenylpropanoid apiol—were the only essential oils that exceeded the 75% inhibition threshold against all three pest species while simultaneously achieving 100% tick larval mortality. The consistently superior potency of *P. mituense* over both *P. sancti-felicis* and pure apiol across all bioassays provides evidence for synergistic contributions from minor constituents, particularly myristicin, bicyclogermacrene, and germacrene D. Principal component analysis confirmed that the chemical class of the dominant constituent determines biocidal selectivity: apiol-rich chemotypes exhibited the strongest broad-spectrum activity, while sesquiterpene-dominated oils conferred taxon-selective effects of lower magnitude. The absence of nematicidal activity against *M. javanica* defines a useful selectivity window for IPM applications. Apiol exhibits favorable binding interactions with acetylcholinesterase and cytochrome P450 enzymes across multiple arthropod species. Its interaction with catalytic residues and its ability to form additional stabilizing contacts support its potential as a bioactive compound.

These findings fill a significant knowledge gap for apiol, previously unexplored as an antifeedant or ixodicidal agent, and extend the biocidal profile of these Amazonian *Piper* chemotypes beyond their previously reported antifungal and herbicidal activities, positioning apiol-rich essential oils as promising dual-purpose candidates for integrated management of crop pests and arthropod vectors of public health concern.

Supplementary Materials: The following supporting information can be downloaded at the website of this paper posted on Preprints.org, Table S1: GC-MS analysis (% abundance) of ten Amazonian Piper species

 doi:10.20944/preprints202605.1475.v1

essential oils. Species abbreviations are: Pa (P. anonifolium), Pcs (P. casapiense), Pc (P. coruscans), Pd (P. dumosum), Pm (P. mituense), Po (P. obliquum), Pr (P. reticulatum), Psf (P. sancti-felicis), Ps (P. soledadense), Pt (P. tuberculatum). Tentative identification of compounds without match (>90%) in the databases have been carried out based on retention time, m/z and retention index. Excel file can be access at DOI: 10.5281/zenodo.20284642. Table S2: Nematicidal activity of Piper oils and apiol against Meloidogyne javanica juveniles (J2). Table S3: Molecular docking results for apiol and reference ligands across acetylcholinesterase (AChE) and cytochrome P450 (CYP450) enzymes. Docking scores correspond to the most favorable pose among 50 generated conformations. Interaction types (hydrogen bonding, π–π stacking, hydrophobic, and polar contacts) were assigned based on residue chemical properties and spatial proximity within the binding pocket.

Author Contributions: Conceptualization, L.R.V. and A.G.C.; funding acquisition, L.R.V. and A.G.C.; investigation, A.G.C., L.R.M., M.F.A.Y., F.V. and W.R.M.; methodology, L.R.V., M.D.J.V.M., D.T., H.R.C., A.G.C., M.F.A.Y. and L.R.M.; writing—original draft, L.R.V. and A.G.C.; writing—review & editing, A.G.C. and L.R.V. All authors have read and agreed to the published version of the manuscript.

Funding: This work was financed by FONDECYT-CONCYTEC (Basic Research Grant N° 433 ,2019, FONDECYT) and Universidad Nacional de la Amazonía Peruana (RR N° 0449, 2024, UNAP), Peru. This research was also funded by Grant PID 2024-156361OB-C22 (State Research Agency, Spain, 10.13039/501100011033).

Institutional Review Board Statement: Not applicable.

Informed Consent Statement: Not applicable.

Data Availability Statement: The original contributions presented in this study are included in the article. Further inquiries can be directed to the corresponding authors.

Acknowledgments: We thank Juan Ruiz for his support in the collection of plant species, and Rubén Molina for his assistance with sample analysis by gas chromatography–mass spectrometry (GC–MS). All authors have readand agreed to the published version of the manuscript.

Conflicts of Interest: The authors declare no conflicts of interest.

References

1. Hawkins, N.J.; Bass, C.; Dixon, A.; Neve, P. The Evolutionary Origins of Pesticide Resistance. *Biol Rev Camb Philos Soc* **2019**, *94*, 135–155, doi:10.1111/brv.12440.
2. Moustafa, M.A.M.; Moteleb, R.I.A.; Ghoneim, Y.F.; Hafez, S.S.; Ali, R.E.; Eweis, E.E.A.; Hassan, N.N. Monitoring Resistance and Biochemical Studies of Three Egyptian Field Strains of *Spodoptera Littoralis* (Lepidoptera: Noctuidae) to Six Insecticides. *Toxics* **2023**, *11*, doi:10.3390/toxics11030211.
3. Bass, C.; Puinean, A.M.; Zimmer, C.T.; Denholm, I.; Field, L.M.; Foster, S.P.; Gutbrod, O.; Nauen, R.; Slater, R.; Williamson, M.S. The Evolution of Insecticide Resistance in the Peach Potato Aphid, *Myzus Persicae*. *Insect Biochem Mol Biol* **2014**, *51*, 41–51, doi:10.1016/j.ibmb.2014.05.003.
4. Gong, P.; Li, X.; Gao, H.; Wang, C.; Li, M.; Zhang, Y.; Li, X.; Liu, E.; Zhu, X. Field Evolved Resistance to Pyrethroids, Neonicotinoids, Organophosphates and Macrolides in *Rhopalosiphum padi* (Linnaeus) and Sitobion Avenae (Fabricius) from China. *Chemosphere* **2021**, *269*, 128747, doi:10.1016/j.chemosphere.2020.128747.
5. Wang, K.; Zhao, J.N.; Bai, J.Y.; Shang, Y.Z.; Zhang, S.Q.; Hou, Y.F.; Chen, M.H.; Han, Z.J. Pyrethroid Resistance and Fitness Cost Conferred by the Super-Kdr Mutation M918L in *Rhopalosiphum padi* (Hemiptera: Aphididae). *J Econ Entomol* **2021**, *114*, 1789–1795, doi:10.1093/jee/toab117.
6. González, J.; Sánchez, M.; Olmeda, Á.S.; Métras, R. *Hyalomma lusitanicum*. *Trends in Parasitology* **2026**, *42*, 140–141, doi:10.1016/j.pt.2025.09.001.
7. Prioritizing Diseases for Research and Development in Emergency Contexts Available online: https://www.who.int/activities/prioritizing-diseases-for-research-and-development-in-emergency-contexts (accessed on 18 March 2026).
8. Eslava, M.; Carlos, S.; Reina, G. Crimean-Congo Hemorrhagic Fever Virus: An Emerging Threat in Europe with a Focus on Epidemiology in Spain. *Pathogens* **2024**, *13*, 770, doi:10.3390/pathogens13090770.

 doi:10.20944/preprints202605.1475.v1

9. Lorenzo Juanes, H.M.; Carbonell, C.; Sendra, B.F.; López-Bernus, A.; Bahamonde, A.; Orfao, A.; Lista, C.V.; Ledesma, M.S.; Negredo, A.I.; Rodríguez-Alonso, B.; et al. Crimean-Congo Hemorrhagic Fever, Spain, 2013-2021. *Emerg Infect Dis* **2023**, *29*, 252–259, doi:10.3201/eid2902.220677.
10. Showler, A.T.; Saelao, P. Integrative Alternative Tactics for Ixodid Control. *Insects* **2022**, *13*, doi:10.3390/insects13030302.
11. Isman, M.B. Plant Essential Oils for Pest and Disease Management. *Crop Protection* **2000**, *19*, 603–608, doi:10.1016/S0261-2194(00)00079-X.
12. Pavela, R.; Benelli, G. Essential Oils as Ecofriendly Biopesticides? Challenges and Constraints. *Trends Plant Sci* **2016**, *21*, 1000–1007, doi:10.1016/j.tplants.2016.10.005.
13. Jankowska, M.; Rogalska, J.; Wyszkowska, J.; Stankiewicz, M. Molecular Targets for Components of Essential Oils in the Insect Nervous System—A Review. *Molecules* **2017**, *23*, doi:10.3390/molecules23010034.
14. Khursheed, A.; Rather, M.A.; Jain, V.; Wani, A.R.; Rasool, S.; Nazir, R.; Malik, N.A.; Majid, S.A. Plant Based Natural Products as Potential Ecofriendly and Safer Biopesticides: A Comprehensive Overview of Their Advantages over Conventional Pesticides, Limitations and Regulatory Aspects. *Microbial Pathogenesis* **2022**, *173*, 105854, doi:10.1016/j.micpath.2022.105854.
15. Duque, J.E.; Urbina, D.L.; Vesga, L.C.; Ortiz-Rodríguez, L.A.; Vanegas, T.S.; Stashenko, E.E.; Mendez-Sanchez, S.C. Insecticidal Activity of Essential Oils from American Native Plants against *Aedes aegypti* (Diptera: Culicidae): An Introduction to Their Possible Mechanism of Action. *Sci Rep* **2023**, *13*, 2989, doi:10.1038/s41598-023-30046-8.
16. Pavela, R.; Kovaříková, K.; Novák, M. Botanical Antifeedants: An Alternative Approach to Pest Control. *Insects* **2025**, *16*, doi:10.3390/insects16020136.
17. Koul, O. Phytochemicals and Insect Control: An Antifeedant Approach. *Critical Reviews in Plant Sciences* **2008**, *27*, 1–24, doi:10.1080/07352680802053908.
18. Jaramillo, M.A.; Manos, P.S. Phylogeny and Patterns of Floral Diversity in the Genus *Piper* (Piperaceae). *Am J Bot* **2001**, *88*, 706–716.
19. Durant-Archibold, A.A.; Santana, A.I.; Gupta, M.P. Ethnomedical Uses and Pharmacological Activities of Most Prevalent Species of Genus *Piper* in Panama: A Review. *Journal of Ethnopharmacology* **2018**, *217*, 63–82, doi:10.1016/j.jep.2018.02.008.
20. da Silva, J.K.; da Trindade, R.; Alves, N.S.; Figueiredo, P.L.; Maia, J.G.S.; Setzer, W.N. Essential Oils from Neotropical Piper Species and Their Biological Activities. *Int J Mol Sci* **2017**, *18*, doi:10.3390/ijms18122571.
21. Bernard, C.B.; Krishanmurty, H.G.; Chauret, D.; Durst, T.; Philogène, B.J.; Sánchez-Vindas, P.; Hasbun, C.; Poveda, L.; San Román, L.; Arnason, J.T. Insecticidal Defenses of Piperaceae from the Neotropics. *J Chem Ecol* **1995**, *21*, 801–814, doi:10.1007/BF02033462.
22. Durofil, A.; Radice, M.; Blanco-Salas, J.; Ruiz-Téllez, T. Piper Aduncum Essential Oil: A Promising Insecticide, Acaricide and Antiparasitic. A Review. *Parasite* **2021**, *28*, 42, doi:10.1051/parasite/2021040.
23. Andrés, M.F.; Rossa, G.E.; Cassel, E.; Vargas, R.M.F.; Santana, O.; Díaz, C.E.; González-Coloma, A. Biocidal Effects of *Piper hispidinervum* (Piperaceae) Essential Oil and Synergism among Its Main Components. *Food Chem Toxicol* **2017**, *109*, 1086–1092, doi:10.1016/j.fct.2017.04.017.
24. Ruiz-Vásquez, L.; Mesia, L.R.; Ceferino, H.D.C.; Mesia, W.R.; Andrés, M.F.; Díaz, C.E.; Gonzalez-Coloma, A. Antifungal and Herbicidal Potential of *Piper* Essential Oils from the Peruvian Amazonia. *Plants* **2022**, *11*, doi:10.3390/plants11141793.
25. Ninkuu, V.; Aluko, O.O.; Yan, J.; Zeng, H.; Liu, G.; Zhao, J.; Li, H.; Chen, S.; Dakora, F.D. Phenylpropanoids Metabolism: Recent Insight into Stress Tolerance and Plant Development Cues. *Front. Plant Sci.* **2025**, *16*, doi:10.3389/fpls.2025.1571825.
26. Zhu, Z.; Chen, R.; Zhang, L. Simple Phenylpropanoids: Recent Advances in Biological Activities, Biosynthetic Pathways, and Microbial Production. *Nat Prod Rep* **2024**, *41*, 6–24, doi:10.1039/d3np00012e.
27. Razzaghi-Abyaneh, M.; Yoshinari, T.; Shams-Ghahfarokhi, M.; Rezaee, M.-B.; Nagasawa, H.; Sakuda, S. Dillapiol and Apiol as Specific Inhibitors of the Biosynthesis of Aflatoxin G1 in *Aspergillus parasiticus*. *Biosci Biotechnol Biochem* **2007**, *71*, 2329–2332, doi:10.1271/bbb.70264.

 doi:10.20944/preprints202605.1475.v1

28. B, S.; M, R.; J, A.; P, J.; S, P.M.; L, M.; R, S.; A, D. A Comprehensive Review of Molecular Docking: Principles, Methods, Applications, and Future Directions. *International Journal of Pharmaceutical Sciences* **2025**, *03*, doi:10.5281/zenodo.18062003.
29. Torres, P.H.M.; Sodero, A.C.R.; Jofily, P.; Silva-Jr, F.P. Key Topics in Molecular Docking for Drug Design. *Int J Mol Sci* **2019**, *20*, 4574, doi:10.3390/ijms20184574.
30. OPLS4. *Schrödinger*.
31. Segura-Navarro, M.J.; Quílez del Moral, J.F.; Andrés, M.F.; Valcárcel, F.; González-Coloma, A.; Molina Inzunza, D.O.; Barrero, A.F. Major Components of *Dittrichia viscosa* (Asteraceae) as a Source of New Pesticides. *Molecules* **2025**, *30*, 3950, doi:10.3390/molecules30193950.
32. Nararak, J.; Sanguanpong, U.; Sukkanon, C.; Manguin, S.; Chareonviriyaphap, T. Synergistic Repellent and Irritant Effects of a Mixture of β-Caryophyllene Oxide and Vetiver Oil against Mosquito Vectors. *Insects* **2023**, *14*, 773, doi:10.3390/insects14090773.
33. Cárdenas-Ortega, N.C.; González-Chávez, M.M.; Figueroa-Brito, R.; Flores-Macías, A.; Romo-Asunción, D.; Martínez-González, D.E.; Pérez-Moreno, V.; Ramos-López, M.A. Composition of the Essential Oil of *Salvia ballotiflora* (Lamiaceae) and Its Insecticidal Activity. *Molecules* **2015**, *20*, 8048–8059, doi:10.3390/molecules20058048.
34. Nararak, J.; Giorgio, C.D.; Sukkanon, C.; Mahiou-Leddet, V.; Ollivier, E.; Manguin, S.; Chareonviriyaphap, T. Excito-Repellency and Biological Safety of β-Caryophyllene Oxide against Aedes Albopictus and *Anopheles dirus* (Diptera: Culicidae). *Acta Trop* **2020**, *210*, 105556, doi:10.1016/j.actatropica.2020.105556.
35. Zheng, R.; Zhao, J.; Ma, L.; Qie, X.; Yan, X.; Hao, C. Behavioral, Electrophysiological, and Toxicological Responses of *Plutella xylostella* to Extracts from *Angelica pubescens*. *Insects* **2023**, *14*, 613, doi:10.3390/insects14070613.
36. Govindarajan, M.; Benelli, G. Eco-Friendly Larvicides from Indian Plants: Effectiveness of Lavandulyl Acetate and Bicyclogermacrene on Malaria, Dengue and Japanese Encephalitis Mosquito Vectors. *Ecotoxicol Environ Saf* **2016**, *133*, 395–402, doi:10.1016/j.ecoenv.2016.07.035.
37. Pavela, R.; Kovaříková, K.; Novák, M. Botanical Antifeedants: An Alternative Approach to Pest Control. *Insects* **2025**, *16*, 136, doi:10.3390/insects16020136.
38. Mladenović, M.; Arsić, B.B.; Stanković, N.; Mihović, N.; Ragno, R.; Regan, A.; Milićević, J.S.; Trtić-Petrović, T.M.; Micić, R. The Targeted Pesticides as Acetylcholinesterase Inhibitors: Comprehensive Cross-Organism Molecular Modelling Studies Performed to Anticipate the Pharmacology of Harmfulness to Humans In Vitro. *Molecules* **2018**, *23*, 2192, doi:10.3390/molecules23092192.
39. Thapa, S.; Lv, M.; Xu, H. Acetylcholinesterase: A Primary Target for Drugs and Insecticides. *Mini Rev Med Chem* **2017**, *17*, 1665–1676, doi:10.2174/1389557517666170120153930.
40. Murray, M. Mechanisms of Inhibitory and Regulatory Effects of Methylenedioxyphenyl Compounds on Cytochrome P450-Dependent Drug Oxidation. *Curr Drug Metab* **2000**, *1*, 67–84, doi:10.2174/1389200003339270.
41. Nauen, R.; Bass, C.; Feyereisen, R.; Vontas, J. The Role of Cytochrome P450s in Insect Toxicology and Resistance. *Annu Rev Entomol* **2022**, *67*, 105–124, doi:10.1146/annurev-ento-070621-061328.
42. Ye, M.; Nayak, B.; Xiong, L.; Xie, C.; Dong, Y.; You, M.; Yuchi, Z.; You, S. The Role of Insect Cytochrome P450s in Mediating Insecticide Resistance. *Agriculture* **2022**, *12*, 53, doi:10.3390/agriculture12010053.
43. Chandor-Proust, A.; Bibby, J.; Régent-Kloeckner, M.; Roux, J.; Guittard-Crilat, E.; Poupardin, R.; Riaz, M.A.; Paine, M.; Dauphin-Villemant, C.; Reynaud, S.; et al. The Central Role of Mosquito Cytochrome P450 CYP6Zs in Insecticide Detoxification Revealed by Functional Expression and Structural Modelling. *Biochem J* **2013**, *455*, 75–85, doi:10.1042/BJ20130577.
44. Murray, M. Toxicological Actions of Plant-Derived and Anthropogenic Methylenedioxyphenyl-Substituted Chemicals in Mammals and Insects. *J Toxicol Environ Health B Crit Rev* **2012**, *15*, 365–395, doi:10.1080/10937404.2012.705105.
45. Hamada, H.M.; Awad, M.; El, -Hefny M.; Moustafa, M. a. M. Insecticidal Activity of Garlic (*Allium sativum*) and Ginger (*Zingiber officinale*) Oils on the Cotton Leafworm, Spodoptera Littoralis (Boisd.) (Lepidoptera: Noctuidae). *African Entomology* **2018**, *26*, 84–94, doi:10.4001/003.026.0084.

 doi:10.20944/preprints202605.1475.v1

46. Valcárcel, F.; Olmeda, A.S.; González, M.G.; Andrés, M.F.; Navarro-Rocha, J.; González-Coloma, A. Acaricidal and Insect Antifeedant Effects of Essential Oils From Selected Aromatic Plants and Their Main Components. *Front. Agron.* **2021**, *3*, doi:10.3389/fagro.2021.662802.
47. Massuh, Y.; Cruz-Estrada, A.; González-Coloma, A.; Ojeda, M.S.; Zygadlo, J.A.; Andrés, M.F. Nematicidal Activity of the Essential Oil of Three Varieties of *Tagetes minuta* from Argentina. *Natural Product Communications* **2017**, *12*, 1934578X1701200515, doi:10.1177/1934578X1701200515.
48. Ruiz-Vásquez, L.; Olmeda, A.S.; Zúñiga, G.; Villarroel, L.; Echeverri, L.F.; González-Coloma, A.; Reina, M. Insect Antifeedant and Ixodicidal Compounds from Senecio Adenotrichius. *Chemistry & Biodiversity* **2017**, *14*, e1600155, doi:10.1002/cbdv.201600155.
49. Hornung, R.W.; Reed, L.D. Estimation of Average Concentration in the Presence of Nondetectable Values. *Applied Occupational and Environmental Hygiene* **1990**, *5*, 46–51, doi:10.1080/1047322X.1990.10389587.
50. Lubin, J.H.; Colt, J.S.; Camann, D.; Davis, S.; Cerhan, J.R.; Severson, R.K.; Bernstein, L.; Hartge, P. Epidemiologic Evaluation of Measurement Data in the Presence of Detection Limits. *Environ Health Perspect* **2004**, *112*, 1691–1696, doi:10.1289/ehp.7199.